Biomass Conversion and Biorefinery (2025) 15:5839–5850
https://doi.org/10.1007/s13399-024-05375-x

ORIGINAL ARTICLE

Green synthesis of silver nanoparticles from waste *Vigna mungo* plant and evaluation of its antioxidant and antibacterial activity

Deepjyoti Mazumder[1,2] · Rishi Mittal[3] · Suresh K. Nath[1]

Received: 24 November 2023 / Revised: 16 January 2024 / Accepted: 26 January 2024 / Published online: 13 February 2024

Abstract

The development of nanoparticles by using bioresources has become a good practice recently to avoid hazardous chemicals and processes. The present study reports the synthesis of silver nanoparticles by using an alkaline food additive prepared from *Vigna mungo* plant waste ash. This food additive called "Khar" is very popular in Assam, a North-Eastern state of India. This additive was used as the reducing and stabilizing agent for the synthesis of silver nanoparticles which were then characterized using TEM, XRD, UV–visible spectroscopy, DLS and zeta potential study, FESEM, and EDX. To study the antioxidant activity of the silver nanoparticle and plant waste ash extract, phytochemical analysis was done using standard methods. The quantitative phytochemical analysis revealed the presence of phenolic and flavonoid compounds in the aqueous extract of the *Vigna mungo* ash which was responsible for the strong antioxidant activity of both ash extracts (IC_{50} = 27.83 µg/mL) and silver nanoparticles (IC_{50} = 13.74 µg/mL). The agar well diffusion method was used for the analysis of the antibacterial activity of silver nanoparticles which showed remarkable antibacterial activity against both the gram-positive bacteria (*Staphylococcus aureus*) and gram-negative bacteria (*Escherichia coli*) respectively. Thus, the study reveals the utility of a traditional food additive made of Assam in the synthesis of silver nanoparticle with notable antioxidant and antibacterial activity.

Keywords Black gram lentil · Silver nanoparticle · Antibacterial · Antioxidant · Food additive · Khar

1 Introduction

The synthesis of silver nanoparticles has gained importance recently due to their wide applicability in anticancer, antibacterial, antimicrobial, catalytic, and anti-inflammatory applications [1]. Therefore, it is of utmost necessity that the preparation method be sustainable, using low-cost materials, natural catalysts, plant-based materials, and other waste materials under mild reaction conditions. Thus, the greener method for synthesis in chemistry refers to less or no use of hazardous chemicals, low power consumption, the production of fewer byproducts, etc. Hence, the biosynthesis of silver nanoparticles has been tried by many researchers and established numerous methods utilizing natural materials such as microorganisms, biological fermentation broth, or plant extracts [1, 2].

Plant-based materials are becoming significant for the synthesis of silver nanoparticles because of the presence of phytochemicals that serve as reducing and stabilizing agents. Even the biological activity of silver nanoparticles was found to be increased when the synthesis was carried out using plant materials [1, 2]. Since they are of low cost and nanoparticles can be produced through simple processes, plant materials or extracts may be taken as valued substitutes for large-scale production of nanoparticles. Therefore, researchers from different regions of the world have tried to synthesize nanoparticles using fruits, leaves, heartwood, roots, seeds of different plants or extracts of those plant parts, and also various bacteria as well as algae [3]. Some examples are *Camellia sinensis, Medicago sativa*, *Cymbopogon flexuosus*, *Pinus desiflora*, *Diospyros kaki*, *Dillenia indica, Ginko biloba*, *Magnolia Kobus, Zingiber officinale, Platanus orientalis* leaf broths, *Platycodon grandiflorum*, *Capsicum annuum* L. extract, *Manilkara zapota,*

✉ Suresh K. Nath
nathsuresh2009@gmail.com

[1] Dept. of Chemistry, Kokrajhar Govt. College, Kokrajhar, BTR, Assam, India 783370

[2] Dept. of Chemistry, Bodoland University, Kokrajhar, BTR, Assam, India 783370

[3] Dept. of Environmental Science and Engineering, Guru Jambheshwar University of Science and Technology, Hisar, Haryana, India 125011

Euphorbia hirta, Bacillus cereus, Staphylococcus aureus, *Acalypha indica* and *Moringa oleifera* leaf extract, *Solanum lycopersicums*, etc. [3–7]. Since the plant materials have proved themselves as good reducing agents for the synthesis of nanoparticles, scientists have tried to use agricultural waste in this area of research [8–11]. A bottom-up approach, i.e., reduction of silver, nucleation, and growth is used for the synthesis of silver nanoparticles using plant extract and agricultural waste extract [8].

Agricultural waste is considered a profitable source for different value-added products, contributing to a zero-waste economy. They are eco-friendly, non-toxic, and low-cost, their extracts can also be used, and they do not generate new pollutants [8, 9]. Synthesis of silver nanoparticles has been done by using different agricultural wastes, e.g., fruit and vegetable-waste extracts, sugarcane bagasse and sweet sorghum bagasse, cereal waste, etc. [8, 10, 12]. In those works, the extract of the wastes was used; however, corn cob waste was burned and the water extract of the ash was used to synthesize CuO nanoparticles [13]. Similarly, in the present study, the authors have used a water extract of ash prepared from agricultural waste for the synthesis of silver nanoparticles.

India is a major production hub for Black gram lentils (*Vigna mungo*) which are cultivated at about 1.82 million tons annually. It helps in cholesterol reduction in humans and animals, and the coat of the seed also has phytochemicals like polyphenols, flavonoids, and phytosterols with different benefits for health [14]. In Assam, a northeastern state of India, the Bodo tribe and other non-tribal communities regularly cultivate Black gram lentils. The plant part is separated from the seed and burned thoroughly after drying, and the ash is used for the preparation of a food additive. The water extract of this ash is highly alkaline, having a pH of 10.94 and it is an alternative to "SODA" or $NaHCO_3$. The reason for the alkalinity is due to the presence of higher concentrations of Na ~ 169.87 ppm and K ~ 323.25 ppm [15]. Traditionally, people use it as an antacid and for other digestive disorders; for cleaning a freshly cut injury from bacterial attack, washing clothes, and as a natural shampoo. Farmers use it for some cattle diseases and to prevent leeches' attacks. This ash extract, locally known as *Khar* has been extensively used as a food additive since ancient times [16–19].

In this work, the plant waste ash extract of Black gram lentils is used as a stabilizing agent for the fabrication of silver nanoparticles. The water extract of the ash is highly alkaline, which is a good condition for the synthesis process. Further, the method is very simple, economical, and sustainable. The synthesized nanoparticles are characterized using UV, FTIR, XRD, DLS, zeta potential, FESEM, EDX, and TEM techniques. The antioxidant capacity was evaluated by the DPPH (*2,2-diphenyl-1-picrylhydrazyl*) free radical scavenging assay, and gram-positive bacteria (*Staphylococcus aureus*) and gram-negative bacteria (*Escherichia coli*) were used in this study to investigate the antibacterial activity of silver nanoparticles.

2 Materials and methods

2.1 Preparation of plant extract

The plants of *Vigna mungo* after harvesting have no marketable value, so the native villagers remove soil particles, clean them properly, and dry them under the sunlight. The dried plants were then burned to ashes and preserved for the preparation of water extracts from them. They used to sell the spare number of ashes and the water extract of the ashes on the market, from where those were purchased. However, they used a tube well or tape water for the preparation of the extract, which is why the extract was prepared in the laboratory using double-distilled water for analytical purposes. A certain quantity of ash was selected after trying to match the pH of the extract available on the market and it was suspended in double-distilled water [15]. After 24 h, it was filtered with Whatman filter paper No. 1 and the resultant ash extract obtained was stored in an airtight container for further use. The pH of the ash extract was found to be 10.94 which depicts its strong alkaline nature. For the synthesis of silver nanoparticles, analytical grade $AgNO_3$ was selected as a precursor, and it was obtained from Thermo Fischer Scientific of 99.98% pure, and DPPH, gallic acid, ascorbic acid, quercetin, methanol, agar, bacteria, and other chemicals were also used as such.

2.2 Synthesis of silver nanoparticles

For the synthesis of silver nanoparticles, 90 mL of 1 mM $AgNO_3$ solution and 10 mL of 100 g/L *Vigna mungo* ash extract were taken, and the latter was added dropwise under vigorous stirring for 6 h at 60 °C [20]. The volume of the solutions was selected after a rigorous trial, following the literature [20]. From the literature, the pH of the extract was found to be ideal for the synthesis of silver nanoparticles with high stability and yield, and it also helps in getting a spherical shape [20]. The conversion of the color of the reaction mixture from light yellow to dark brown due to the reduction of Ag^+ to silver nanoparticles provided visual confirmation [21]. The reaction mixture was incubated for the next 24 h at room temperature to completely reduce silver ions, followed by centrifuging it at 4000 rpm for 15 min. The precipitate was then collected and washed thoroughly several times with ethanol, followed by double-distilled water, dried, and stored for further analysis [22, 23].

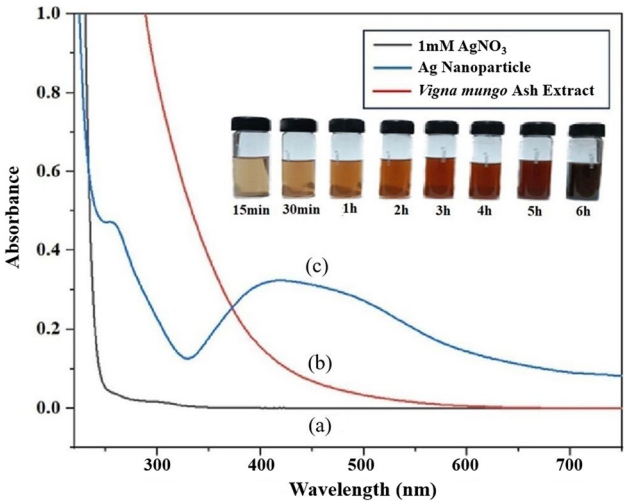

Fig. 1 UV–visible analysis of (a) $AgNO_3$, (b) *Vigna mungo* ash extract, and (c) silver nanoparticle

2.3 Characterization of silver nanoparticles

For the UV–Vis spectrum, the synthesized silver nanoparticles were diluted 20 times into Millipore water and recorded using the UV–Vis Spectrophotometer Model No. UV-2600 230 V. The functional groups were responsible for the reduction of Ag^+ to nano-Ag and the stabilization of nanoparticles was characterized using FTIR and compared with the FTIR spectra of *Vigna mungo,* using the FTIR spectrophotometer Perkin Elmer spectrum model. The Malvern Nano-ZS90 model was used to conduct zeta potential and dynamic light scattering (DLS) analysis to determine the surface charge and size of the nanoparticles. For DLS and zeta potential measurement, 0.01 g of powdered AgNPs was dispersed into 100 mL DMSO at room temperature [24]. Tunneling electron microscopy (TEM) analysis was performed using JEM-2100 PLUS (HR), JEOL for the determination of the shape and size of nanoparticles. The surface morphology of the synthesized silver nanoparticles was analyzed by Image J software. X-ray diffraction was performed using Benchtop Miniflex-II, Rigaku, Japan, at a wavelength of 1.54056 A° at 27 °C, ranging from 20 to 80° (2θ), and the crystallite size of the nanoparticles was calculated using the Debye–Scherrer equation [1, 2]. The surface morphology of the synthesized silver nanoparticle was investigated by field emission scanning electron microscopy (FESEM) analysis using model-7610F plus/JEOL, and the elemental composition was carried out by energy dispersive X-ray spectroscopic (EDX) analysis.

2.4 Phytochemical analysis and quantification of total phenolic and flavonoid content

The phytochemicals such as polyphenols, flavonoids, phytosterols, terpenoids, amino acids, and carbohydrates were tested for the aqueous ash extract of *Vigna mungo* following standard methods [25]. The total phenolic content (TPC) of the ash extract of *Vigna mungo* was determined by Folin-Ciocalteu assay using gallic acid as a standard. Ash extract and the Folin-Ciocalteu reagent were mixed properly, followed by sodium carbonate, and incubated until it gave a blue color, and the absorbance was recorded at 760 nm. The total flavonoid content (TFC) of the ash extract of *Vigna mungo* was determined using the aluminum chloride colorimetric method using quercetin as a standard. Aluminum trichloride, sodium acetate, and ash extracts of various concentrations were mixed in equal volumes, and distilled water was added after that. The mixture was shaken vigorously, and 30 min of incubation was done at room temperature before the absorbance was recorded at 415 nm [25].

2.5 DPPH (2,2-diphenyl-1-picrylhydrazyl) free radical scavenging assay

The DPPH free radical activity was performed for *Vigna mungo* ash extract and silver nanoparticles using the standard method [26]. Separately, 1 mL of each of the different concentrations of ash extract and silver nanoparticles was mixed with 3 mL methanolic solution of DPPH and incubated for 30 min in the dark followed by measuring the absorbance at λ_{max} = 517 nm. Ascorbic acid was used as standard in this experiment, and the blank solution was prepared by adding 3 mL of methanol to 1 mL of DPPH. The percentage inhibition of the ash extract and silver nanoparticles was calculated using the standard formula for the absorbance of a blank solution and a mixture of a plant extract and silver nanoparticles [27].

$$\%\text{inhibition} = \frac{(Ac - As)}{As} \times 100$$

where A_c is the absorbance of blank or control, A_s is the absorbance of plant extract and silver nanoparticle mixture or standard.

2.6 Antibacterial activity of synthesized silver nanoparticles

The agar well diffusion method was used for the analysis of antibacterial activity against both gram-positive bacteria (*Staphylococcus aureus*) and gram-negative bacteria (*Escherichia coli*)

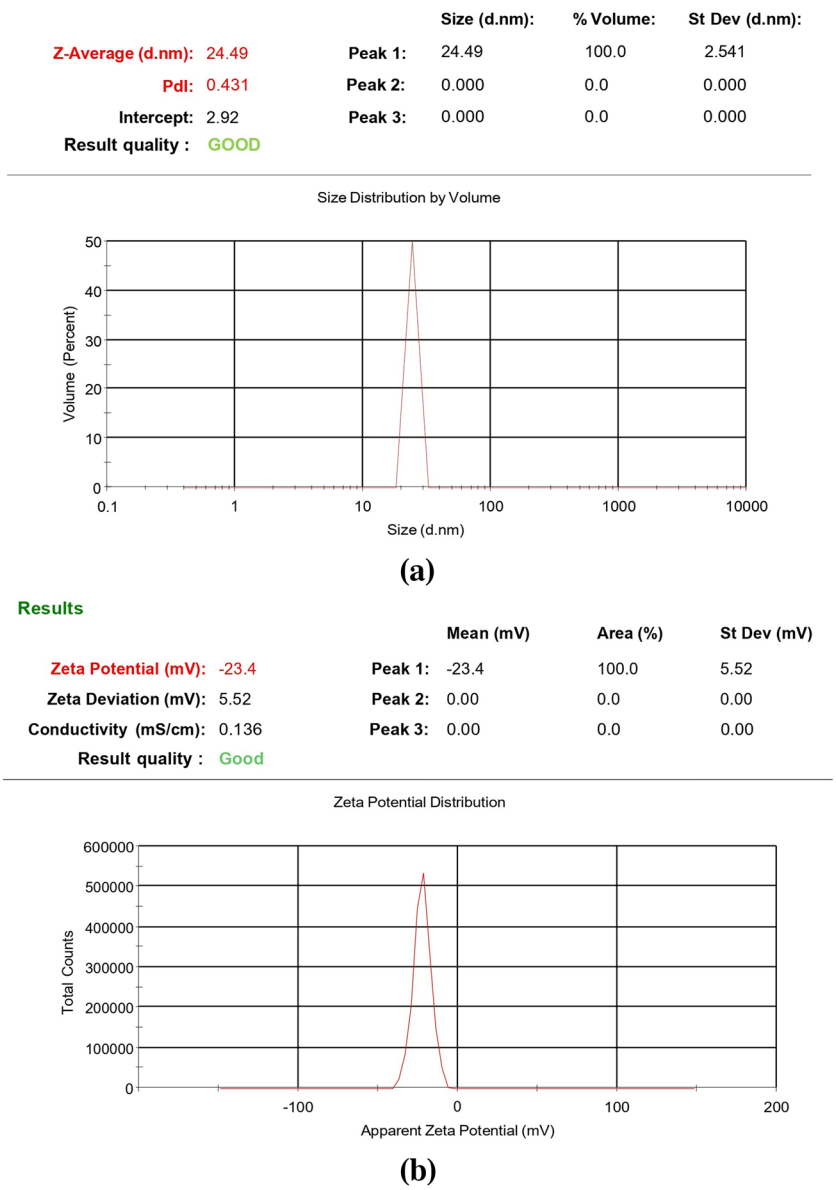

Fig. 2 **a** DLS analysis of silver nanoparticles using *Vigna mungo* ash extract. **b** Zeta potential of the synthesized silver nanoparticles

[28]. The plate count agar and nutrient agar (medium) were dissolved in distilled water, sterilized in an autoclave for 15 min at 121 °C at 15 psi, and then cooled at room temperature. After pouring the agar medium into Petri plates, it was allowed to cool at room temperature until it solidified, and then it was inoculated with a standardized solution of *Staphylococcus aureus* and *Escherichia coli*, respectively. A 100 µL sterilized tip was used to prepare wells in the Petri plates, and 25 mg/mL, 50 mg/mL, and 75 mg/mL ultrasonicated nanoparticle solutions were inoculated. After 24 h of incubation at 37 °C, the zone of inhibition was measured using a ruler [29]. Standard plates were made with ampicillin (10 mg), penicillin (10 mg), and vancomycin (30 mg).

3 Results and discussion

3.1 UV–visible analysis

As silver nanoparticles form, the color of the reaction mixture changes from pale yellow to dark brown, indicating the development, and stabilization of the nanoparticles, as seen in Fig. 1. According to previous reports, silver nanoparticles have absorption bands of 400–450 nm [3]. The absorption band for surface plasmonic resonance (SPR) at 436 nm indicates the growth of well-dispersed nanoparticles that are not forming aggregates. This may be due to the presence of excess ligands, blocking agents, and the formation of the ellipsoidal shape of the particles [30]. Since the extract has chloride, the absorption band is lowered, which may be due

Table 1 Crystallite size measured from XRD data

Parameters			Calculations		
K	λ (A°)	Peak position 2θ (°)	FWHMβ (°)	*D* (nm)	Average *D* (nm)
		38.07	0.35	24.0108959	
0.94	1.5406	44.22	0.75	11.43314507	23.300
		64.535	0.36	26.09790463	
		76.701	0.32	31.65641401	

to the formation of silver chloride-containing nanoparticles [31].

3.2 FT-IR analysis

FT-IR spectroscopy can aid in recognizing the bioactive molecules that participate in the nucleation of Ag metals and stabilizing them [32]. Therefore, the FT-IR spectra of the biosynthesized silver nanoparticle have been compared with the spectra of *Vigna mungo* ash to identify the functional groups that are responsible for the reduction and stabilization of the synthesized nanoparticles [23]. A broad peak has appeared at 3440 cm^{-1} in the spectra of silver nanoparticles and at 3447 cm^{-1} of the FT-IR spectra of *Vigna mungo* ash, due to the O–H stretching of the protein molecules and polyphenolic molecules such as tannins present in the *Vigna mungo* Ash [33, 34]. The peaks appearing at 2924 cm^{-1} and 2855 cm^{-1} are due to the stretching vibration of the C-H bond [20, 35]. Two intense peaks are observed at 1651 cm^{-1} and 1390 cm^{-1} in the spectra of silver nanoparticle as well as at 1652 cm^{-1} and 1403 cm^{-1} in the spectra of *Vigna mungo* ash due to the C=C aromatic group and primary amide group ($-CONH_2$) of protein molecule respectively. The C–O–C stretching was shown by two strong peaks at 1114 cm^{-1} and another at 1010 cm^{-1} in the fingerprint region of silver nanoparticle spectra. The peak at 982 cm^{-1} corresponds to C=C bending vibration [36]. The aromatic compound C-H bending vibrations were represented by the peak at 832 cm^{-1}, 663 cm^{-1}, and 617 cm^{-1} [20, 37, 38]. Hence, all these mentioned peaks refer to the presence of some functional groups which are part of phytochemicals in the ash of *Vigna Mungo* waste and, they are responsible for nucleation and stabilization of the synthesized silver nanoparticles [36, 38].

3.3 DLS size distribution and zeta potential

The particle size distribution, surface charge, and size of nanoparticles formed can be examined by the dynamic light scattering technique, where the Brownian motion of spherical particles interacts with light. In DLS measurement, a

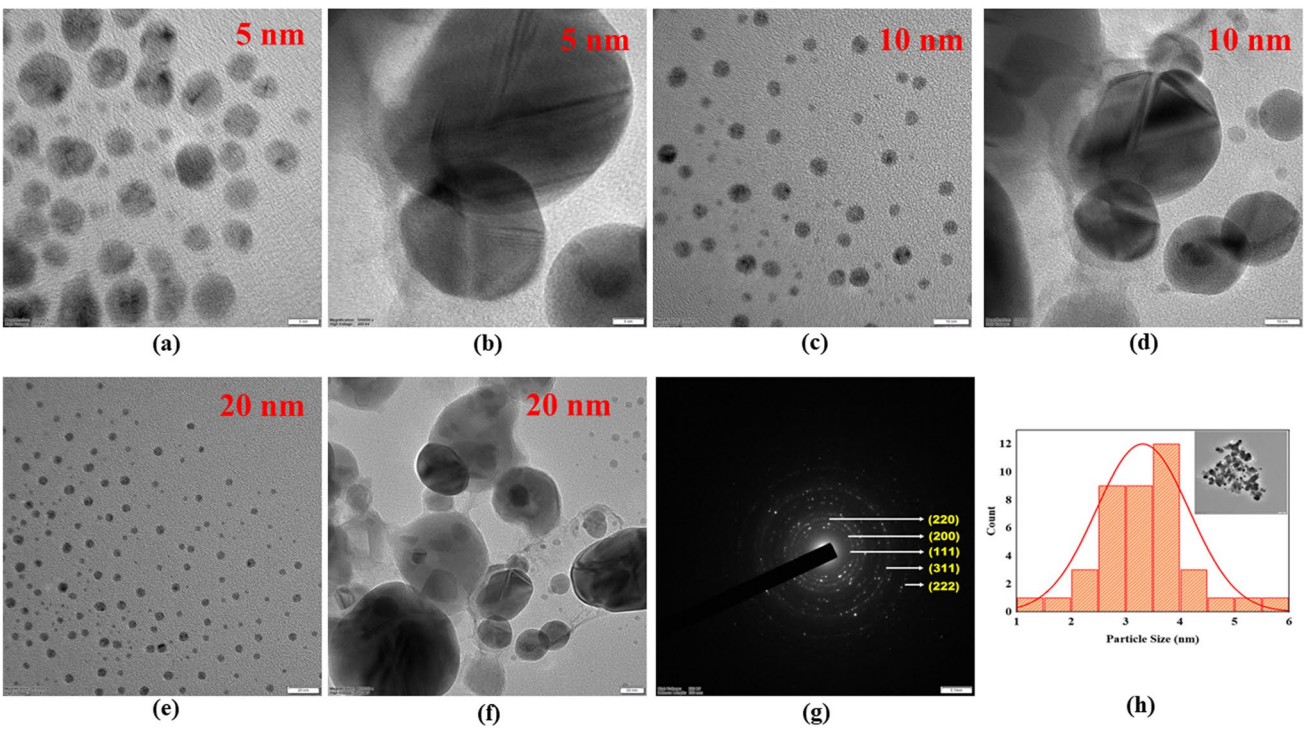

Fig. 3 The TEM images **a**, **b** 5 nm; **c**, **d** 10 nm, and **e**, **f** 20 nm, **g** SAED pattern, **h** particle size distribution

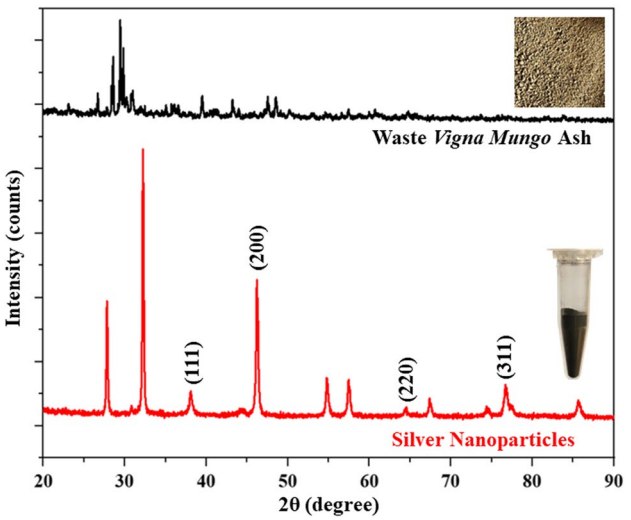

Fig. 4 XRD analysis of *Vigna mungo* ash extract and silver nanoparticle

hydrodynamic sphere is formed in aqueous media around the nanoparticles [32]. The scattered intensities of light are used to determine the hydrodynamic diameter; however, this diameter is affected by electrical layers and stabilizing agents. The polydispersity index provides an idea of particle size distribution; if it is less than 0.1, it is monodispersed, and if it is greater than 0.7, there is a broad particle size distribution in the sample [39]. DLS analysis showed that the average mean particle size of biosynthesized silver nanoparticles was 24.49 nm. However, the mean size of the nanoparticle obtained from DLS analysis tends to be larger than that obtained from electron microscopy. This is because of the hydrodynamic sphere formed in aqueous media around the nanoparticles, leading to their larger size (Fig. 2a) [40]. The polydispersity index (PDI) of the biosynthesized nanoparticles was found to be 0.431, which is below 0.7, indicating that the nanoparticles were slightly aggregated [24].

The electrostatic interaction of nanoparticles can be scaled by using zeta potential, and it predicts the stability of the dispersion system. According to previous works, a colloidal solution having a zeta potential value in the range of − 30 to + 30 mV is considered to be very stable [41, 42]. The zeta potential of silver nanoparticles was negatively charged and had a value of − 23.4 mV (Fig. 2b). In the work of silver nanoparticle synthesis using aloe vera extracts, Muhammad Riaz et al. mentioned the performance of capping agents on stabilizing nanoparticles about the value of zeta potential [43]. A high negative zeta potential value indicates that the colloidal

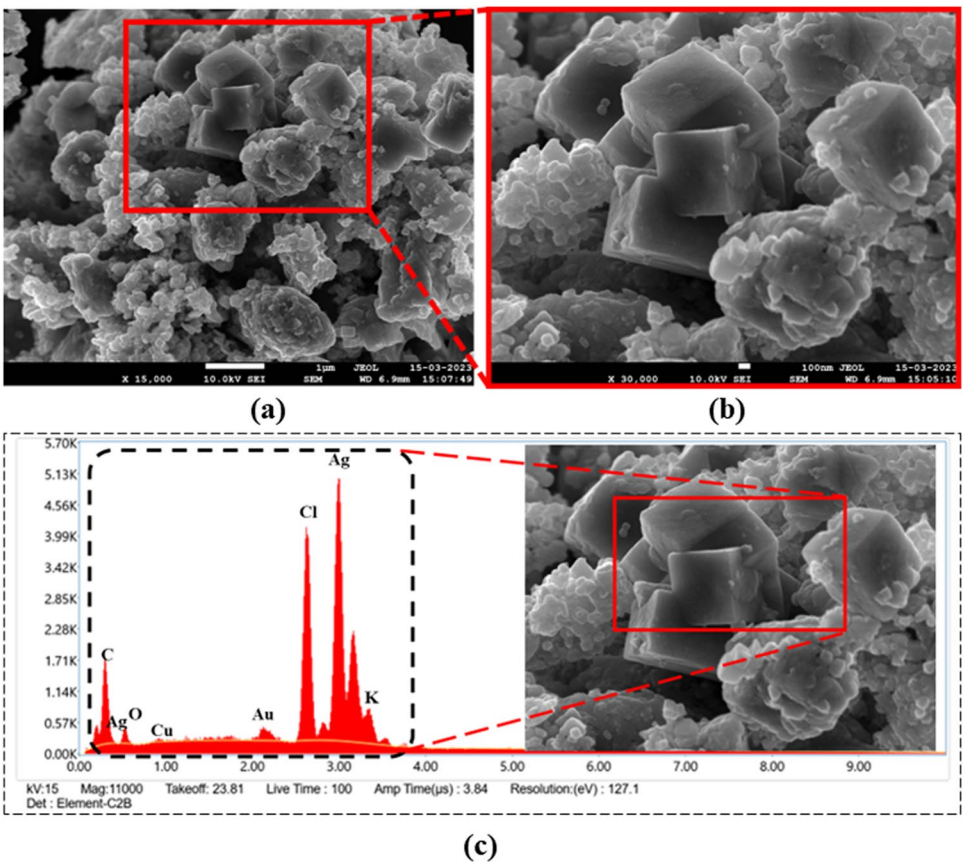

Fig. 5 FESEM images at different magnifications. **a** 1 μm, **b** 100 nm, and **c** EDX of silver nanoparticles

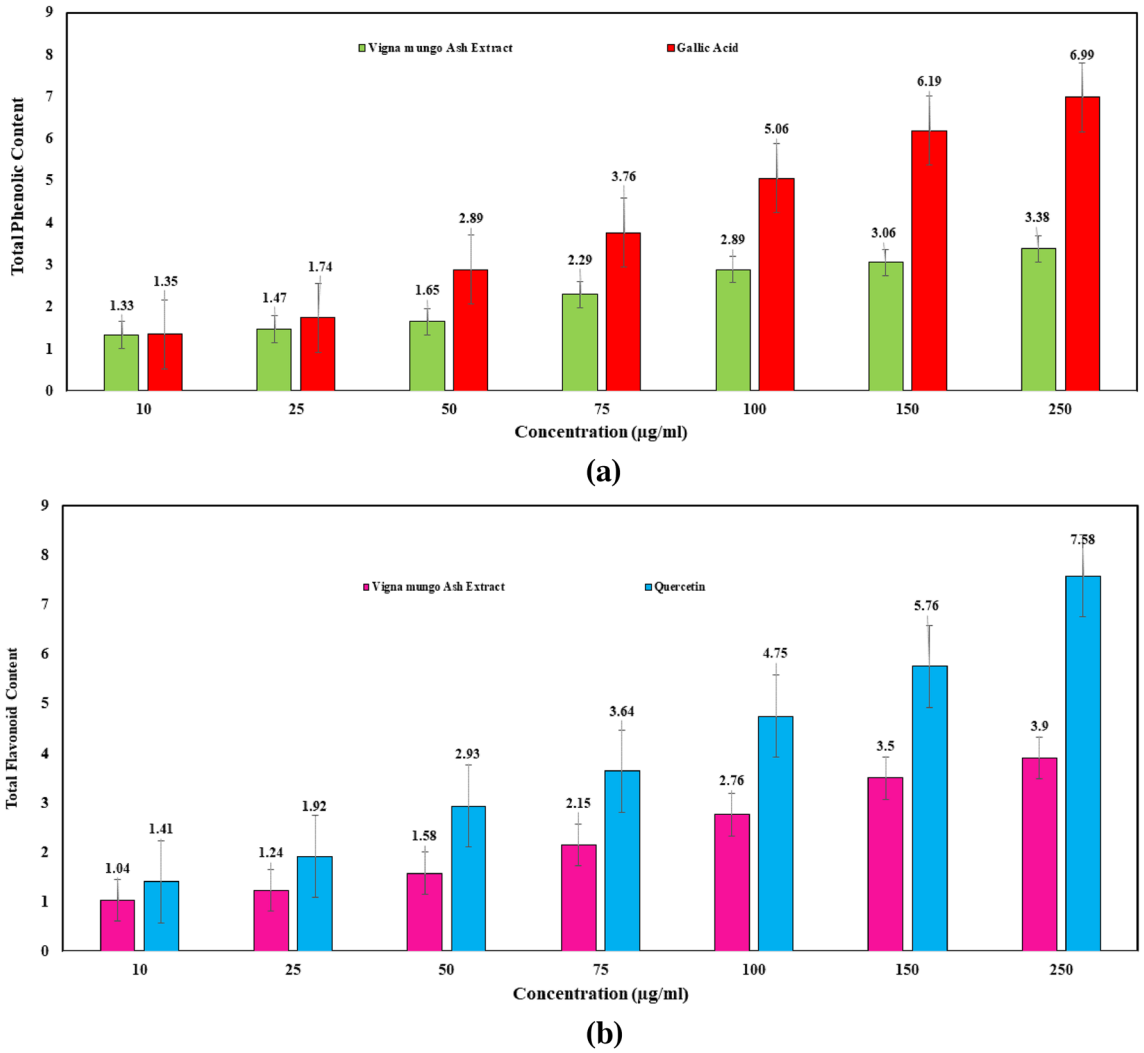

Fig. 6 **a** Total phenolic content of *Vigna mungo* ash extract. **b** Total flavonoid content of *Vigna mungo* ash extract

suspension of synthesized nanoparticles is highly stable as those have been capped by the phytochemicals present in the plant extract [32, 44]. The colloidal solution with high zeta potential experiences strong repulsive forces which prevent them from coming into contact and aggregating [45–47].

3.4 TEM analysis

The average size and surface morphology of the synthesized silver nanoparticles were determined by using high-resolution TEM. Figure 3 represents the TEM images, particle size distribution, and selected area electron diffraction (SAED) pattern. The nanoparticles were mostly spherical, as observed in Fig. 3 and b at 5 nm, (c, d) at 10 nm, and (e, f) at 20 nm. The size distribution histogram in Fig. 3g revealed that the size is mostly in the 2–6 nm range. However, from DLS analysis, it has been observed that the average size is 24.49 nm, which is due to the hydrodynamic sphere produced by the phytochemicals. The SAED pattern of silver nanoparticles given in Fig. 3h had some brilliant, bright circular rings, indicating the nanoparticles' crystalline nature as reported by Song and Kim [48]. The (111), (200), (220), and (311) planes of silver nanoparticles matched with the circular rings of the SAED pattern [39, 40]. It can also be observed that most of the nanoparticles are scattered; only a few particles are in a little agglomerate formation.

3.5 X-ray diffraction analysis

The *Vigna mungo* plant ash extract mediated synthesized colloidal silver nanoparticles were centrifuged and dried for XRD study. The X-ray diffraction pattern is demonstrated in Fig. 4. In this diffractogram, the peaks appear at 38.07°, 44.22°, 64.535°, and 76.701° for 2θ values

corresponding to (111), (200), (220), and (311) crystallographic planes, respectively, which matched the values established earlier by [43]. Those values also specify the face-centered cubic structure of *Vigna mungo* ash extract-mediated silver nanoparticles. In addition to these peaks, there were some other peaks also observed in the diffractogram that appeared due to the presence of phytochemicals in the plant ash extract [22, 49]. The average crystallite size of synthesized nanoparticles was also determined by using Scherrer's equation, and it was found to be 23.30 nm [40] (Table 1). This size matched the result of the DLS analysis; however, in the TEM analysis, the result was different, i.e., 2–6 nm. This difference is because of the hydrodynamic sphere produced by the phytochemicals, as established by [40].

3.6 FESEM analysis

The FESEM analysis was done to investigate the synthesized silver nanoparticles' surface morphology and EDX analysis to determine the elemental composition. The FESEM image showed that there is an agglomeration of some smaller nanoparticles which results in the formation of some bigger-sized silver nanoparticle agglomerates of roughly spherical shape as seen in (Fig. 6). Apart from this, FESEM images showed some bigger size perfect cube-shaped silver nanoparticles. This wide range of shapes and sizes of the synthesized nanoparticles may be attributed to the different phytochemicals present in the plant ash extract, which act differently in the formation of the nanoparticles [8, 50]. In Fig. 5c, a sharp peak at 3 keV in in the EDX pattern of the synthesized silver nanoparticles validated the presence of elemental silver which confirmed the successful synthesis of silver nanoparticles using *Vigna mungo* ash extract. Apart from this, there were some other peaks for Cl, C, K, O, and Cu present in the EDX pattern which came from plant ash extract [20].

3.7 Phytochemical analysis of *Vigna mungo* ash extract

The variety of phytochemical compounds present in the *Vigna mungo* ash extract are phenolic compounds, tannins, phlobatannins, carbohydrates, alkaloids, and flavonoids. Compounds such as cardiac glycosides, steroids, amino acids, fixed oils and fats, glycosides, phytosterols, saponins, gums and mucilage, and terpenoids were not detected. The total phenolic and flavonoid contents of the aqueous ash extract are affected by the quantity of ash, as shown in Fig. 6a and b [25, 51]. At a maximum concentration of 250 µg/mL ash extract, the total phenolic content was found to be 3.38 ± 0.033 µg/ml, and the total flavonoid content was 3.90 ± 0.054 µg/mL, respectively. The phenolic acid-mediated nanoparticle synthesis gives higher antioxidant activity to the particles [52]. Further, the FTIR spectra analysis of *Vigna mungo* and silver nanoparticles provides information on the functional groups present in the phytochemicals (Fig. 7).

3.8 DPPH Antioxidant Assay

The antioxidant activity of silver nanoparticles and ash extract in contrast to ascorbic acid (standard) has been shown in Fig. 8. The antioxidant activity was monitored by a change in the color of the solution from violet to yellow due to the formation of diphenyl picryl hydrazine [26]. The percent of DPPH scavenging activity of nanoparticles was in the range

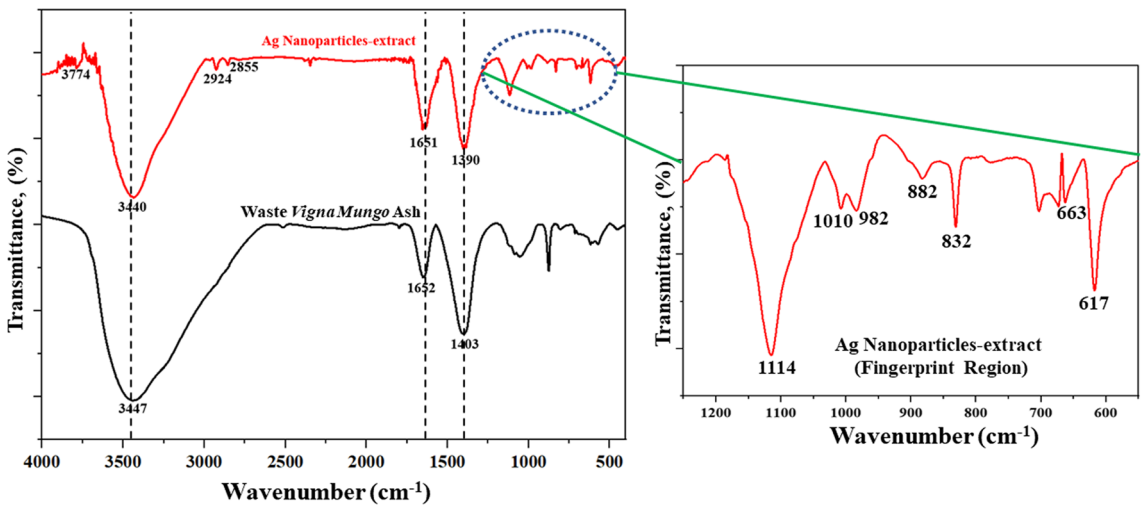

Fig. 7 FTIR analysis of silver nanoparticles and *Vigna mungo* ash

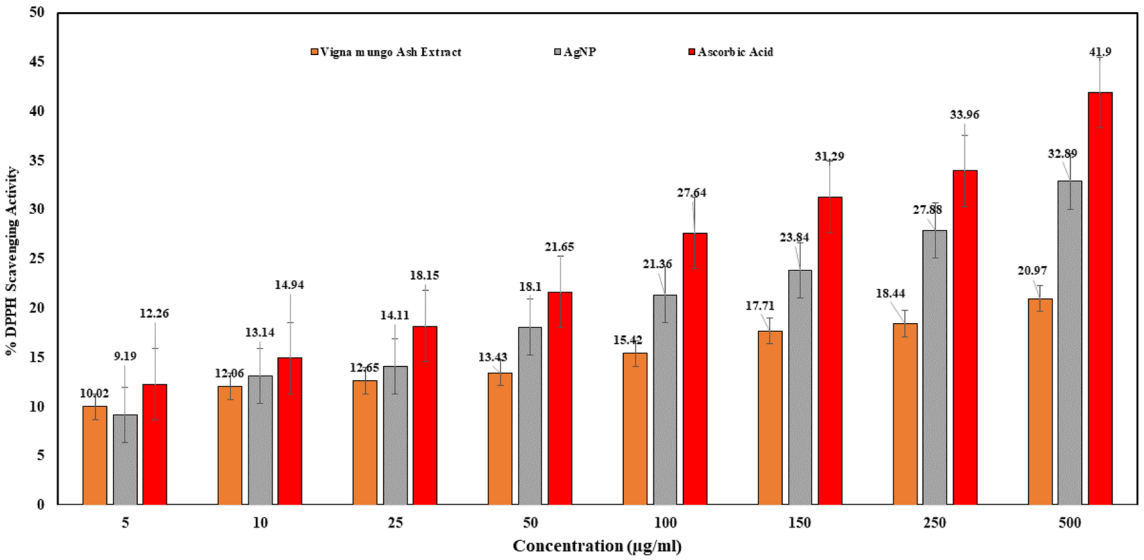

Fig. 8 Estimation of the DPPH radical scavenging activity

of 9.19 ± 0.13 to 32.89 ± 0.29%. For the ash extract, when the concentration varies from 5 to 500 µg/mL, the scavenging activity was 10.02 ± 0.21 to 20.97 ± 0.71% whereas for ascorbic acid it was 12.26 ± 0.23 to 41.99 ± 0.13%. The half-maximal inhibitory concentration (IC_{50}) values were determined from the regression analysis graph. They were found to be 13.74 µg/mL for synthesized silver nanoparticles, 27.83 µg/mL for ash extract, and 10.48 µg/mL for ascorbic acid, respectively. The synthesized silver nanoparticles showed high antioxidant activity, which may be due to the phytochemicals present in ash extract, particularly the flavonoids present on their surface that inhibit the free radicals [53].

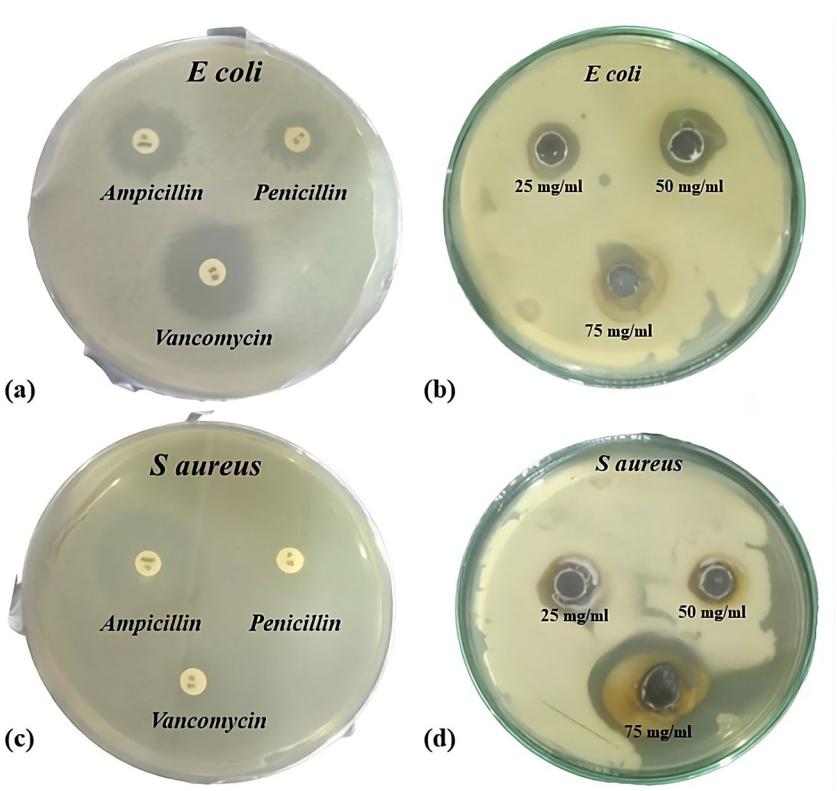

Fig. 9 Antibacterial activity of the synthesized silver nanoparticles against **a** standard, **b** gram-negative bacteria (*Escherichia coli*), **c** standard, and **d** gram-positive bacteria (*Staphylococcus aureus*)

3.9 Antibacterial activity analysis

The results of the agar well diffusion method to test the antibacterial activity of the synthesized silver nanoparticles against gram-positive bacteria (*Staphylococcus aureus*) and gram-negative bacteria (*Escherichia coli*) have been displayed in Fig. 9. With the increase in concentration and decrease in size of the nanoparticles, the antibacterial activity was enhanced [20].

In this study, *Staphylococcus aureus* had a greater zone of inhibition than *Escherichia coli*, indicating that the nanoparticles were more efficient against *Staphylococcus aureus* (Table 2 and 3). In this study, for a higher concentration of nanoparticles, a higher zone of inhibition was found. The very small size of 2–6 nm silver nanoparticles was capable of penetrating through the bacterial cell walls, interacting with cytochromes, and disturbing the electron transport process. Nanoparticles also produce reactive oxygen species leading to the disturbance in respiration and energy transfer process causing death of the bacterial cell [50, 54, 55].

4 Conclusion

This study adopted a green reducing agent, i.e., an aqueous extract of *Vigna mungo* plant ash for the synthesis of silver nanoparticles which is a popular food additive in Assam, India. The advantage of the synthesis route is that it employs an agricultural waste-derived food additive for a simple, affordable, green, and environmentally favorable method for the synthesis. According to the TEM analysis, the average diameter of synthesized silver nanoparticles was 2–6 nm having spherical morphology. Several other techniques viz., UV–visible spectroscopy, FT-IR, XRD, FESEM, EDX, SAED, DLS particle size, and zeta potential analyzer have supported the synthesized nanoparticles to be spherical, stable with very little agglomeration. The phytochemicals present in the extract helped the formation and stabilization of nanoparticles. The antioxidant activity of silver nanoparticles was greatly enhanced in comparison to the plant extract in the DPPH assay. They exhibited high antibacterial potential towards both gram-positive (*Staphylococcus aureus*) and gram-negative bacteria (*Escherichia coli*) due to their extremely small size. Thus, it can be concluded here that, an agricultural waste-derived alkaline food additive, may be applied for the synthesis of nanoparticles without using any other reagents, and it can have potential antioxidant and antibacterial activity. However, there is a scope for the further improvement of the properties of synthesized nanoparticles, using raw waste extract.

Acknowledgements The authors thank Sophisticated Analytical Instrumentation Centre (SAIC), Institute of Advanced Study in Science and Technology (IASST), Guwahati, DST, Government of India, for TEM analysis and Dept. of Environmental Science and Engineering, Guru Jambheshwar University of Science and Technology, Hisar, Haryana, India for XRD, FT-IR, ZETA, and DLS analyses.

Author contribution Deepjyoti Mazumder: investigation, formal analysis, visualization, writing—original draft; Rishi Mittal: investigation, formal analysis; Suresh Kumar Nath: conceptualization, writing—original draft, methodology, validation, supervision, visualization.

Data availability Not applicable.

Declarations

Ethics approval Not applicable

Competing interests The authors declare no competing interests.

Table 2 Observed zone of inhibition for synthesized silver nanoparticle

	25 mg/mL	50 mg/mL	75 mg/mL
Escherichia coli	14.67 ± 0.59 mm	17.67 ± 0.65 mm	19 ± 0.95 mm
Staphylococcus aureus	13 ± 0.58 mm	17.33 ± 0.55 mm	20 ± 0.95 mm

Table 3 Observed zone of inhibition of standard

Serial no	Standard name	*Escherichia coli*	*Staphylococcus aureus*
1	Ampicillin (10 mg)	12.33 ± 0.59 mm	20 ± 0.57 mm
2	Penicillin (10 mg)	7.67 ± 0.65 mm	6 ± 0.58 mm
3	Vancomycin (30 mg)	18.33 ± 0.33 mm	4.67 ± 0.55 mm

References

1. Nie P, Zhao Y, Xu H (2023) Synthesis, applications, toxicity and toxicity mechanisms of silver nanoparticles: a review. Ecotoxicol Environ Saf 253. https://doi.org/10.1016/j.ecoenv.2023.114636
2. Tian S, Saravanan K, Mothana RA et al (2020) Anti-cancer activity of biosynthesized silver nanoparticles using Avicennia marina against A549 lung cancer cells through ROS/mitochondrial damages. Saudi J Biol Sci 27:3018–3024. https://doi.org/10.1016/j.sjbs.2020.08.029
3. Soliman MKY, Abu-Elghait M, Salem SS, Azab MS (2022) Multifunctional properties of silver and gold nanoparticles synthesis by Fusarium pseudonygamai. Biomass Convers Biorefin. https://doi.org/10.1007/s13399-022-03507-9
4. Baran Ayşe et al (2022) Investigation of antimicrobial and cytotoxic properties and specification of silver nanoparticles (AgNPs) derived from Cicer arietinum L. green leaf extract. Front Bioeng Biotechnol 10:855136. https://doi.org/10.3389/fbioe.2022.855136
5. Ramazanli VN, Ahmadov IS (2022) "Synthesis of silver nanoparticles by using extract of olive leaves." Adv Biol Earth Sci 7(3):238–244

6. Gunashova GY (2022) Synthesis of silver nanoparticles using a thermophilic bacterium strain isolated from the spring Yukhari istisu of the Kalbajar region (Azerbaijan). Adv Biol Earth Sci 7(3):198–204
7. Sharma A, Mittal R et al (2023) Sustainable approach for adsorptive removal of cationic and anionic dyes by titanium oxide nanoparticles synthesized biogenically using algal extract of spirulina. Nanotechnology 34:485301. https://doi.org/10.1088/1361-6528/acf37e
8. Rodríguez-Félix F, Graciano-Verdugo AZ, Moreno-Vásquez MJ et al (2021) Trends in sustainable green synthesis of silver nanoparticles using agri-food waste extracts and their applications in health. J Nanomater 2022:37. https://doi.org/10.1155/2022/8874003
9. Baran A, Baran MF, Keskin C et al (2021) Ecofriendly/rapid synthesis of silver nanoparticles using extract of waste parts of artichoke (Cynara scolymus L.) and evaluation of their cytotoxic and antibacterial activities. J Nanomater 10:855136. https://doi.org/10.3389/fbioe.2022.855136
10. Saha P, Kim BS (2022) Chapter 11: Plant extract and agricultural waste-mediated synthesis of silver nanoparticles and their biochemical activities. Green Synthesis of Silver Nanomaterials. Nanobiotechnology for Plant Protection: Elsevier, pp 285–315. https://doi.org/10.1016/B978-0-12-824508-8.00010-1
11. Baran A et al (2021) Ecofriendly/rapid synthesis of silver nanoparticles using extract of waste parts of artichoke (Cynara scolymus L.) and evaluation of their cytotoxic and antibacterial activities. J Nanomater 2021:1–10. https://doi.org/10.1155/2021/2270472
12. Mythili R, Selvankumar T, Kamala-Kannan S et al (2018) Utilization of market vegetable waste for silver nanoparticle synthesis and its antibacterial activity. Mater Lett 225:101–104. https://doi.org/10.1016/j.matlet.2018.04.111
13. Torres-Arellano S, Torres-Martinez LM, Luévano-Hipólito E et al (2023) Biologically mediated synthesis of CuO nanoparticles using corn COB (Zea mays) ash for photocatalytic hydrogen production. Mater Chem Phys 301:127640. https://doi.org/10.1016/J.MATCHEMPHYS.2023.127640
14. Arockianathan PM, Rajalakshmi K, Nagappan1 P (2019) Proximate composition, phytochemicals, minerals and antioxidant activities of Vigna mungo L. seed coat. Bioinformation 15:579–585. https://doi.org/10.6026/97320630015579
15. Mazumder D, Narzary A, Nath SK (2023) Chemical composition, characterization and antioxidant property of a food additive prepared from Vigna mungo (black gram lentils) plant waste. Indian J Nutr Diet 60:378–388. https://doi.org/10.21048/IJND.2023.60.3.33129
16. Kalita D, Deb B (2004) Some folk medicines used by the Sonowal Kacharis tribe of the Brahmaputra valley, Assam. Natural Product Radiance 3:240–246. https://nopr.niscpr.res.in/bitstream/123456789/9438/1/NPR%203(4)%20240-246.pdf
17. Hussain A, Khan MN et al (2010) In vitro screening of the leaves of Musa paradisiaca for anthelmintic activity. J Animal Plant Sci 20:5–8. https://www.researchgate.net/publication/225298346. Accessed Jul 2023
18. Mohapatra D, Mishra S, Sutar N (2010) Banana and its by-product utilisation: an overview. J Sci and Ind Res 69:323–329
19. Varsha Kelkar Mane MRH (2014) Analysis of traditional food additive Kolakhar for its physico-chemical parameters and antimicrobial activity. J Food Process Technol 5:1000387–1000388. https://doi.org/10.4172/2157-7110.1000387
20. Sarma PP, Barman K, Baruah PK (2023) Green synthesis of silver nanoparticles using Murraya koenigii leaf extract with efficient catalytic, antimicrobial, and sensing properties towards heavy metal ions. Inorg Chem Commun 152:110676. https://doi.org/10.1016/j.inoche.2023.110676
21. Ramesh PS, Kokila T, Geetha D (2015) Plant mediated green synthesis and antibacterial activity of silver nanoparticles using Emblica officinalis fruit extract. Spectrochim Acta A Mol Biomol Spectrosc 142:339–343. https://doi.org/10.1016/j.saa.2015.01.062
22. Ibrahim HMM (2015) Green synthesis and characterization of silver nanoparticles using banana peel extract and their antimicrobial activity against representative microorganisms. J Radiat Res Appl Sci 8:265–275. https://doi.org/10.1016/j.jrras.2015.01.007
23. Rodríguez-Félix F, López-Cota AG, Moreno-Vásquez MJ et al (2021) Sustainable-green synthesis of silver nanoparticles using safflower (Carthamus tinctorius L.) waste extract and its antibacterial activity. Heliyon 7:4. https://doi.org/10.1016/j.heliyon.2021.e06923
24. Al-Karagoly H, Rhyaf A, Naji H et al (2022) Green synthesis, characterization, cytotoxicity, and antimicrobial activity of iron oxide nanoparticles using Nigella sativa seed extract. Green Processes Synth 11:254–265. https://doi.org/10.1515/gps-2022-0026
25. Ezeonu CS, Ejikeme CM (2016) Qualitative and Quantitative Determination of Phytochemical Contents of Indigenous Nigerian Softwoods. New J of Sci 5601327. https://doi.org/10.1155/2016/5601327
26. Konappa N, Udayashankar AC, Dhamodaran N et al (2021) Ameliorated antibacterial and antioxidant properties by Trichoderma harzianum mediated green synthesis of silver nanoparticles. Biomolecules 11:4. https://doi.org/10.3390/biom11040535
27. Sánchez-Moreno C (2002) Methods used to evaluate the free radical scavenging activity in foods and biological systems. Food Sci Technol Int 8:121–137. https://doi.org/10.1106/108201302026770
28. Balouiri M, Sadiki M, Ibnsouda SK (2016) Methods for in vitro evaluating antimicrobial activity: a review. J Pharm Anal 6:71–79
29. Aritonang HF, Koleangan H, Wuntu AD (2019) Synthesis of silver nanoparticles using aqueous extract of medicinal plants' (impatiens balsamina and Lantana camara) fresh leaves and analysis of antimicrobial activity. Int J Microbiol 2019:1–8. https://doi.org/10.1155/2019/8642303
30. Jaast S, Grewal A (2021) Green synthesis of silver nanoparticles, characterization and evaluation of their photocatalytic dye degradation activity, Current Res in Green Sustain Chem 4:100195. https://doi.org/10.1016/j.crgsc.2021.100195
31. Lou Z, Huang B, Wang P et al (2011) The synthesis of the near-spherical AgCl crystal for visible light photocatalytic applications. Dalton Trans 40:4104–4110. https://doi.org/10.1039/c0dt01795g
32. Alharbi NS, Alsubhi NS (2022) Green synthesis and anticancer activity of silver nanoparticles prepared using fruit extract of Azadirachta indica. J Radiat Res Appl Sci 15:335–345. https://doi.org/10.1016/j.jrras.2022.08.009
33. Jaffar SS, Saallah S, Misson M et al (2023) Green synthesis of flower-like carrageenan-silver nanoparticles and elucidation of its physicochemical and antibacterial properties. Molecules 28:2. https://doi.org/10.3390/molecules28020907
34. Sandulovici RC, Carmen-Marinela M, Grigoroiu A et al (2023) The physicochemical and antimicrobial properties of silver/gold nanoparticles obtained by "green synthesis" from willow bark and their formulations as potential innovative pharmaceutical substances. Pharmaceuticals 16:1. https://doi.org/10.3390/ph16010048
35. Moreno-Vargas JM, Echeverry-Cardona LM, Moreno-Montoya LE, Restrepo-Parra E (2023) Evaluation of antifungal activity of Ag nanoparticles synthetized by green chemistry against Fusarium solani and Rhizopus stolonifera. Nanomaterials 13:3. https://doi.org/10.3390/nano13030548

36. Widatalla HA, Yassin LF, Alrasheid AA et al (2022) Green synthesis of silver nanoparticles using green tea leaf extract, characterization and evaluation of antimicrobial activity. Nanoscale Adv 4:911–915. https://doi.org/10.1039/d1na00509j
37. Chandraker SK, Lal M, Shukla R et al (2019) Colorimetric sensing of Fe^{3+} and Hg^{2+} and photocatalytic activity of green synthesized silver nanoparticles from the leaf extract of: Sonchus arvensis L. New J Chem 43:18175–18183. https://doi.org/10.1039/c9nj01338e
38. Kanniah P, Chelliah P, Thangapandi JR et al (2021) Green synthesis of antibacterial and cytotoxic silver nanoparticles by Piper nigrum seed extract and development of antibacterial silver based chitosan nanocomposite. Int J Biol Macromol 189:18–33. https://doi.org/10.1016/j.ijbiomac.2021.08.056
39. Clayton KN, Salameh JW, Wereley ST, Kinzer-Ursem TL (2016) Physical characterization of nanoparticle size and surface modification using particle scattering diffusometry. Biomicrofluidics 10:054107. https://doi.org/10.1063/1.4962992
40. Alzubaidi AK, Al-Kaabi WJ, Al AA et al (2023) Green synthesis and characterization of silver nanoparticles using flaxseed extract and evaluation of their antibacterial and antioxidant activities. Appl Sci (Switzerland) 13:2182. https://doi.org/10.3390/app13042182
41. Mittal R, Sharma S et al (2023) Removal of chromium (vi) using spirulina assisted mesoporous iron oxide nanoparticles. Ing Chm Communications 154:110881. https://doi.org/10.1016/j.inoche.2023.110881
42. Das P, Dutta T, Manna S et al (2022) Facile green synthesis of non-genotoxic, non-hemolytic organometallic silver nanoparticles using extract of crushed, wasted, and spent Humulus lupulus (hops): characterization, anti-bacterial, and anti-cancer studies. Environ Res 204:111962. https://doi.org/10.1016/j.envres.2021.111962
43. Riaz M, Sharafat U, Zahid N et al (2022) Synthesis of biogenic silver nanocatalyst and their antibacterial and organic pollutants reduction ability. ACS Omega 7:14723–14734. https://doi.org/10.1021/acsomega.1c07365
44. Hemlata MPR, Singh AP, Tejavath KK (2020) Biosynthesis of silver nanoparticles using Cucumis prophetarum aqueous leaf extract and their antibacterial and antiproliferative activity against cancer cell lines. ACS Omega 5:5520–5528. https://doi.org/10.1021/acsomega.0c00155
45. Aryan R, Mehata MS (2021) Green synthesis of silver nanoparticles using Kalanchoe pinnata leaves (life plant) and their antibacterial and photocatalytic activities. Chem Phys Lett 778:138760. https://doi.org/10.1016/j.cplett.2021.138760
46. Khane Y, Benouis K, Albukhaty S et al (2022) Green synthesis of silver nanoparticles using aqueous citrus limon zest extract: characterization and evaluation of their antioxidant and antimicrobial properties. Nanomaterials 12:12. https://doi.org/10.3390/nano12122013
47. Pallavi SS, Rudayni HA, Bepari A et al (2022) Green synthesis of silver nanoparticles using Streptomyces hirsutus strain SNPGA-8 and their characterization, antimicrobial activity, and anticancer activity against human lung carcinoma cell line A549. Saudi J Biol Sci 29:228–238. https://doi.org/10.1016/j.sjbs.2021.08.084
48. Song JY, Kim BS (2009) Rapid biological synthesis of silver nanoparticles using plant leaf extracts. Bioprocess Biosyst Eng 32:79–84. https://doi.org/10.1007/s00449-008-0224-6
49. Rautela A, Rani J, Debnath (Das) M (2019) Green synthesis of silver nanoparticles from Tectona grandis seeds extract: characterization and mechanism of antimicrobial action on different microorganisms. J Anal Sci Technol 10:1-10. https://doi.org/10.1186/s40543-018-0163-z
50. Aboutorabi SN, Nasiriboroumand M, Mohammadi P et al (2018) Biosynthesis of silver nanoparticles using safflower flower: structural characterization, and its antibacterial activity on applied wool fabric. J Inorg Organomet Polym Mater 28:2525–2532. https://doi.org/10.1007/s10904-018-0925-5
51. Jyoti K, Baunthiyal M, Singh A (2016) Characterization of silver nanoparticles synthesized using Urtica dioica Linn. leaves and their synergistic effects with antibiotics. J Radiat Res Appl Sci 9:217–227. https://doi.org/10.1016/j.jrras.2015.10.002
52. Amini SM, Akbari A (2019) Metal nanoparticles synthesis through natural phenolic acids. Natl Libr Med 13:771–777. https://doi.org/10.1049/iet-nbt.2018.5386
53. Yousefbeyk F, Dabirian S, Ghanbarzadeh S et al (2022) Green synthesis of silver nanoparticles from Stachys by zantina K. Koch: characterization, antioxidant, antibacterial, and cytotoxic activity. Part Sci Technol 40:219–232. https://doi.org/10.1080/02726351.2021.1930302
54. Rafique M, Sadaf I, Rafique MS, Tahir MB (2017) A review on green synthesis of silver nanoparticles and their applications. Artif Cells Nanomed Biotechnol 45:1272–1291. https://doi.org/10.1016/j.msec.2019.02.059
55. Rafique M, Sadaf I, Tahir MB et al (2019) Novel and facile synthesis of silver nanoparticles using Albizia procera leaf extract for dye degradation and antibacterial applications. Mater Sci Eng, C 99:1313–1324. https://doi.org/10.1016/j.msec.2019.02.059